Group Velocity Estimation for the Calibration of Localization Algorithms in Lamb Wave SHM Systems

Francesco Falcetelli*
Alma Mater Studiorum Università di Bologna, Forlì, 47121, Italy

Acoustic Emission (AE) is widely used for Structural Health Monitoring (SHM) systems. It is a passive technique with the potential to detect an AE event even if its location is not known a priori. Assessing the correct wave group velocity is fundamental for the performance of localization algorithms based on Lamb waves propagation and can be useful for the setup of numerical models. AE events were generated performing Hsu-Nielsen Pencil-Lead Breaks (PLB) tests, a repeatable emission which can be applied at different regions of the structure. This study focuses on the development of a methodology to calibrate a localization algorithm posing particular attention in the symmetric fundamental mode group velocity estimation. The work was performed as a part of six months research period carried out at Clarkson University, NY, USA.

I. Nomenclature

A_0	=	Antisymmetric Lamb wave mode
S_0	=	Symmetric Lamb wave mode
λ	=	Wavelength
k	=	Wave number
ω	=	Angular frequency
c_L	=	Longitudinal wave velocity (unbounded conditions)
c_T	=	Transverse wave velocity (unbounded conditions)
c_g	=	Group velocity
c_{ph}	=	Phase velocity
c_s	=	S-Wave velocity (shear)
c_p	=	P-Wave velocity (longitudinal)
λ	=	Wavelength
ρ	=	Material density
h	=	Plate half thickness

II. Introduction

In recent years, technology is making great strides in many engineering applications leading to increasingly complex structures. The aerospace industry, driven by an increasing demand for mobility, is trying to manufacture increasingly lighter and safer structures to reduce fuel consumption (minimizing the costs) and keeping sufficiently high safety levels. Structural Health Monitoring (SHM) finds its natural place in this contest, where the capability to detect a damage as soon as possible is a crucial point. According to C.R. Farrar, SHM is referred to as the process of implementing a damage identification strategy for different kind of structures [1].

There are many different techniques within SHM. Many of them are similar to Non-Destructive Evaluation (NDE) methods, with the difference that the monitoring system in SHM is embedded within the structure or performed in-situ while in NDE this is not the case. The first important remark is that SHM techniques can be divided in two families: *passive* and *active* methods [2]. In the passive approach, the monitoring of the structure takes place by

* M.Sc. Aerospace Engineering candidate, francesco.falcetelli@studio.unibo.it

“listening” a change in a sensor signal induced by the damage being generated. On the other hand, active approaches make use of both sensors and actuators. Hence, the structure is excited by the action of the actuators and its response is detected by the sensors. As such, a baseline of data representing the free-damage case is produced and then compared with the system response in presence of damage by means of a piezoelectric sensors network. Acoustic Emissions (AE) falls inside the passive techniques and is often used to develop localization algorithms aiming to detect the AE events originating from failure/damage site.
A localization algorithm is based on the detection of multiple AE events by several piezoelectric transducers. From the knowledge of the recorded time of arrivals (TOA) and the wave speed, the AE source can be successfully identified using a triangulation technique. Nevertheless, even if the algorithm scheme is relatively simple, determining painstakingly those two parameters is an ongoing challenge for many researches. Therefore, there is the need for calibrating the system through experiments using a reproducible AE source. In 1981, Hsu and Nielsen introduced the so-called Pencil-Lead break technique in an attempt to reproduce a real AE source.
The lead of a mechanical pencil, (usually 2H hardness) is pushed against the structure at a defined angle between 20 and 60 degrees. The lead diameter is 0.3 mm but also 0.5 mm leads are accepted if there is the need for a higher amplitude signal. In order to be consistent, it is recommended to use always the same angle, lead diameter and length (typically between 2 and 3 mm) [3].

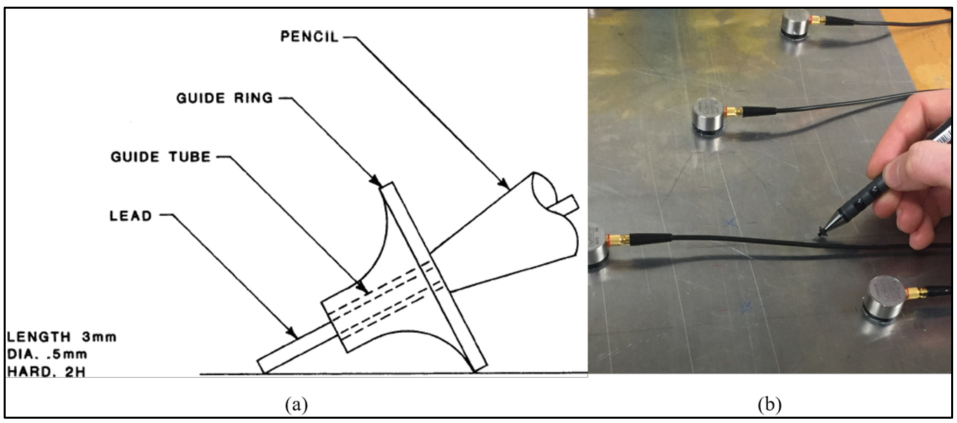

Fig. 1: Pencil Lead Break schematic [3], (a), and during an experiment, (b).

The elastic potential energy is released when the pencil lead breaks generating an AE. Since this experiment can be easily replicated in all common laboratory environments, PLB is a standard tool in many AE studies in order obtain a representative wave speed on that specific structure.
Researchers have been using PLB experiments to characterize the behaviour of AE signals along structures. The frequency and intensity of the different Lamb wave modes, the determination of group velocities, the signal attenuation, the sensor tuning, and the assessment of the source location performance can be performed by means of a PLB test [4].

III. Lamb Waves

Sound waves in solids are, from a conceptual point of view, analogous to the well-known sound waves propagating in the atmosphere. Without going through the equations, it is possible to say that in both cases the problem is characterized by longitudinal waves propagating with a certain speed. The main difference is that solid materials can withstand shear forces, resulting in a second possible type of propagating waves, commonly called transverse waves. The problem of elastic waves travelling in a solid material becomes more complex once a bounded medium is considered. A variety of different wave types can be generated depending on the considered geometry. In the case when only one side is bounded, elastic waves are referred to as Rayleigh waves, while if both sides are bounded (i.e. wave propagating in a plate, or a shell) elastic waves are referred to as Lamb waves.
Lamb waves take their name from Horace Lamb which was the first to discover those kinds of waves in 1917 in his famous work “On Waves in an Elastic Plate” [5]. They are also found in the literature under the name of guided waves in contrast with the aforementioned bulk waves. Those two waves families share the same set of partial differential equations despite of their important differences. What makes the difference are the boundary conditions applied to the mathematical problem when dealing with guided waves. The necessity to satisfy those boundary conditions raises the difficulty of the problem, leading to extremely complex analytical solutions [6].

In order to state the governing equations associated with the propagation of guided waves, a plate which thickness is equal to 2h, as depicted in Fig. 2, is considered.

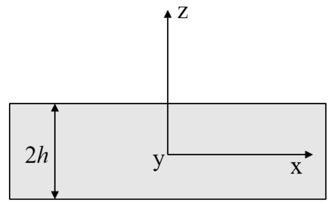

Fig. 2: Coordinate system related to Lamb waves propagating in a plate.

It is possible to show that there are two kinds of solutions describing the propagation of Lamb waves: one in which the in-plane displacement is an even function and another where the in-plane displacement is an odd function. Those solutions are associated with the so-called symmetric and antisymmetric modes respectively [7]. Applying the boundary conditions (i.e. null value of the stress when $y = h$ or $y = -h$), it is possible to obtain the dispersion relations:

$$\frac{\tan(qh)}{\tan(ph)} = -\frac{4k^2pq}{(q^2-k^2)^2} \quad \text{(a);} \quad \frac{\tan(ph)}{\tan(qh)} = -\frac{4k^2pq}{(q^2-k^2)^2} \quad \text{(b)} \tag{1}$$

for the symmetric and antisymmetric solution, respectively. Where,

$$p = -\frac{\omega}{\sqrt{(c_L{}^2-c^2)}} \quad \text{(a);} \quad q = -\frac{\omega}{\sqrt{(c_T{}^2-c^2)}} \quad \text{(b)} \tag{2}$$

As stated previously, h is half of the plate thickness. On the other hand, the wavenumber is denoted by k, the angular frequency with ω, while c_L and c_T represents the longitudinal and transverse wave velocities respectively for unbounded conditions [8]. Equation (1a) and Eq. (1b) show the link between the angular frequency and the associated possible velocities c related to the symmetric and the antisymmetric modes. More precisely, the velocity is linked to the so-called frequency-thickness product ωh. Therefore, those relationships have a physical meaning: Lamb waves, contrary to bulk waves, are strongly dispersive. Not surprisingly Eq. (1a) and Eq. (1b) are also referred as dispersion relations. Those equations can be solved only numerically and are transcendental, meaning that they can lead to many different real solutions which generate correspondingly different symmetric and antisymmetric modes along the frequency domain.
From an experimental point of view is fundamental to understand which Lamb wave modes are present in order to tune properly the group velocity for the localization algorithm. Therefore, after a standard noise test, a preliminary analysis regarding the AE spectrum is required to determine how many modes are present and to understand which is the most suitable to reconstruct the source location.

IV. Experimental setup

The experiments were carried out at the Holistic Structural Integrity Process Laboratory at Clarkson University, NY, USA. The AE signals were analyzed by means of an AMSY-6 system, developed by Vallen Systeme GmbH™.

A. Hardware description

The AMSY-6 is an AE measurement system capable of processing information coming from several channels simultaneously. The measurement chain, representative of an AE channel, starts with a piezoelectric sensor that records an elastic wave at the surface of the monitored structure. The signal is transmitted through a preamplifier, which is connected to the ASIP-2 (double channel Acoustic Signal Processor). Finally, a USB connection transfers to the computer the data related to the AE features extracted by the ASIP-2.

B. Sensors, Preamplifiers and AE Signal Processor

Figure 2 shows the first two elements of the AMSY-6 measurement chain. The VS900-M, represented in Fig. 3 (a), is a piezoelectric sensor characterized by a broadband frequency response. It has a stainless-steel case and its weight is about 22 g. Since it does not support an integrated preamplifier, it is connected the AEP5H, shown in Fig. 3 (b), in order to amplify the signal. The AEP5H is a wide-band preamplifier with a gain that can be set to 34 dB or 40 dB by means of a switch located inside the preamplifier itself.

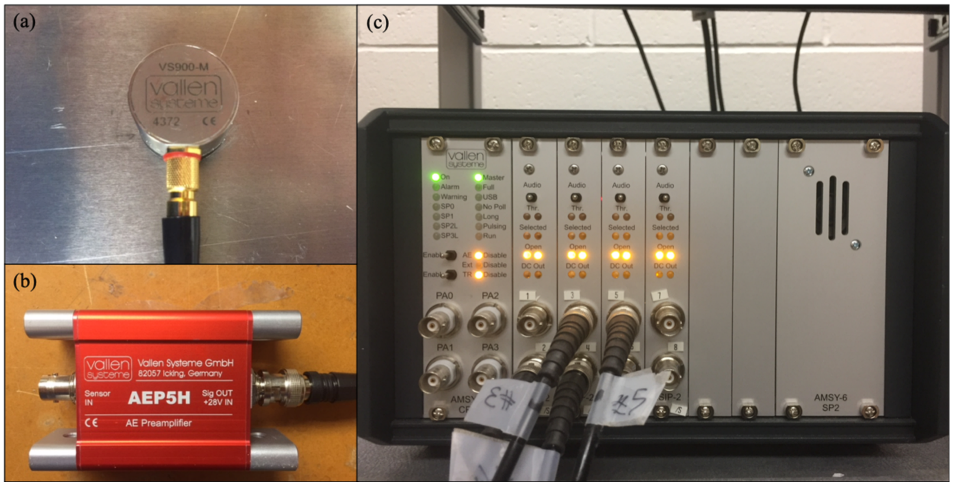

Fig. 3: Piezoelectric sensor VS900-M, (a), and Preamplifier AEP5H, (b), Front view of the MB6 chassis (c).

Figure 3 (c) shows the front view of the ASIP-2 together with the control panel, the parametric input channels. The MB6 chassis holds all the previously mentioned elements together, resulting in a compact configuration.

C. Specimen parameters and first sensor layout

A 7075-T651 aluminum plate, measuring 304.8 mm (X direction) by 609.6 mm (Y direction) by 1.6 mm (thickness), was used in this study. According to the data sheet, the specimen density, ρ, and Young's Modulus, E, were 2810 kg/m^3 and 71.7 GPa respectively.

The material choice was justified by the fact that aluminum alloys are commonly used in aerospace structures. Moreover, it is an isotropic material, leading to circular propagating Lamb waves at the surface of the plate. In the literature, it is common to find Acoustic Emissions studies applied to anisotropic materials such as composites, but this increases the complexity of the problem. The changing of material properties with the direction leads to wave patterns of different shapes, that are difficult to model or to implement for a localization algorithm [9]. This study, which can be considered as the first part of a wider research project, tries to avoid unnecessary increments in complexity, without losing of generality. Table 1 gives the coordinates of the various piezoelectric transducers for this first part of the project where the origin of the used reference system was the south-east corner of the plate and the sensor names were chosen arbitrarily.

Table 1. Sensors coordinates for the experimental layout

General		Coordinates [mm]		Coordinates [in.]	
Sensor	Channel	X	Y	X	Y
1	1	152.4	304.8	6	12
2	2	76.2	457.2	3	18
3	3	228.6	406.4	9	16
4	4	228.6	152.4	9	6
5	5	76.2	203.2	3	8
6	8	152.4	549.7	6	21.6

V. Noise Test

Data acquisition is a crucial point to obtain accurate results. In particular, the selection of the proper threshold value allows the software to select the right time of arrival related to the AE. For this purpose, the noise level affecting the piezoelectric sensors has to be considered. A standard procedure to conduct a noise test is to set the detection threshold to a relatively low value and acquire data for a period of at least 5 minutes. Following this guideline, several noise tests were performed with a threshold of 28.3 dB for each channel. The maximum peak amplitude recorded in the experiments was used as a reference in order to determine the proper threshold value as it is described by the following Eq. (3):

$$Th = N_{max} + X \tag{3}$$

Where Th is the detection threshold, N_{max} is the measured peak amplitude and X is a user defined parameter whose value has to be equal or greater than 6 dB.

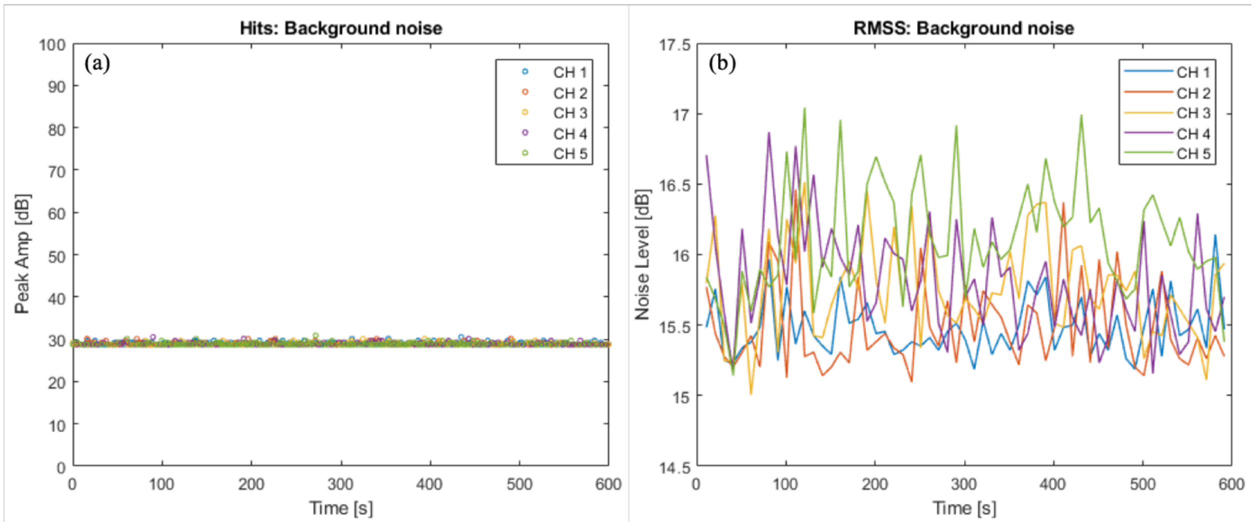

Fig. 4: Hits (a) and noise root-mean square (b) recorded in each channel over 10 minutes.

The recorded hits in Fig. 4 (a) show a measured peak amplitude N_{max} slightly higher than 30 dB. Therefore, taking as a reference N_{max} and giving to X a value of 6 dB, Eq. (3) provides a threshold value equal to 36 dB.
Another way to determine the detection threshold is to use as reference the root-mean square value of the noise in each channel (RMS-status). The RMS-status variable (or RMSS) represents the energy associated with the noise level and is computed by the Vallen software in [μV]. Data are stored in evenly spaced time intervals of 1 second, independently from the threshold crossing. The recorded data were imported in Matlab™ and plotted in dB using the following Eq. (4):

$$RMSS_{dB} = 20 \log [(RMSS_{\mu V})/1\mu V] \tag{4}$$

Usually a minimum value of 20 dB above the steady RMSS value is recommended in order to avoid undesired threshold triggers [10]. In Fig. 4 (b) the RMS-status variable (RMSS) over 10 minutes of recording is shown.
Adding 20 dB to the RMSS steady value, that can be considered around 16 dB (Fig. 4), leads to a threshold value of 36 dB. It is interesting to note that the same result is obtained independently from the method applied, suggesting the reliability of the data. Therefore, 36 dB was taken as an initial threshold setting. After several experiments, with a trial and error approach, it was decided to increase this value up to 38.1 dB in order to avoid any possible undesired hit. A further increase of the value would lead to poor sensitivity of the sensors therefore affecting the quality of the data acquisition process.

VI. PLB Signal and Spectrum characterization

A preliminary study on the PLB signal was carried out in order to assess their main features. The Hsu-Nielsen source represents a repeatable acoustic emission, nevertheless each PLB is unique and slightly different from another one due to the many variables that can potentially affect the generated signal. For practical reasons, is almost impossible to perform experiments applying every time exactly the same pressure on the aluminum plate. Moreover, even using the same pressure the pencil lead could brake sooner or later due to internal defects which cannot be controlled. Applying precisely the same contact angle in each test is another challenging task of a PLB experiment.
Bearing in mind the aforementioned considerations, it was decided to perform the same experiment three times using a 2H 0.3 mm diameter lead with a contact angle of 45 degrees. The choice of using a 0.3 lead is due to the fact that the considered geometry is relatively small, and a 0.5 lead would lead to a higher amplitude signal reaching the sensor

saturation limit of 100 mV. The location of the PLB test has coordinates (152,4 mm; 99,7 mm) whereas the signal was recorded by Sensor 6.
Therefore, the relative distance between the acoustic emission source and the transducer was 450 mm. The results of the three experiments are plotted in Fig. 5 (a). The signal is recorded starting from a user defined number of samples before the first hit by means of the “PreTrg” variable. In this case, the pre-trigger was set equal to 200 samples and since the sampling frequency, f_s, is equal to 5 MHz, as a consequence the Time of Arrival (TOA) has to be necessarily of 40 μs. Therefore, in every experiment made with the Vallen Systeme the first TOA is always equal to 40 μs. Nevertheless, will be shown that the key parameter is not the TOA itself but the difference between the TOA recorded by different sensors. Moreover, according to the Nyquist-Shannon sampling theorem, with a sampling frequency of 5 MHz it is possible to characterize with no aliasing an analog signal with an upper band-limit of 2.5 MHz. In this study, the maximum frequency of interest is not higher than 500 kHz; therefore, the used sampling frequency is more than enough to avoid aliasing.

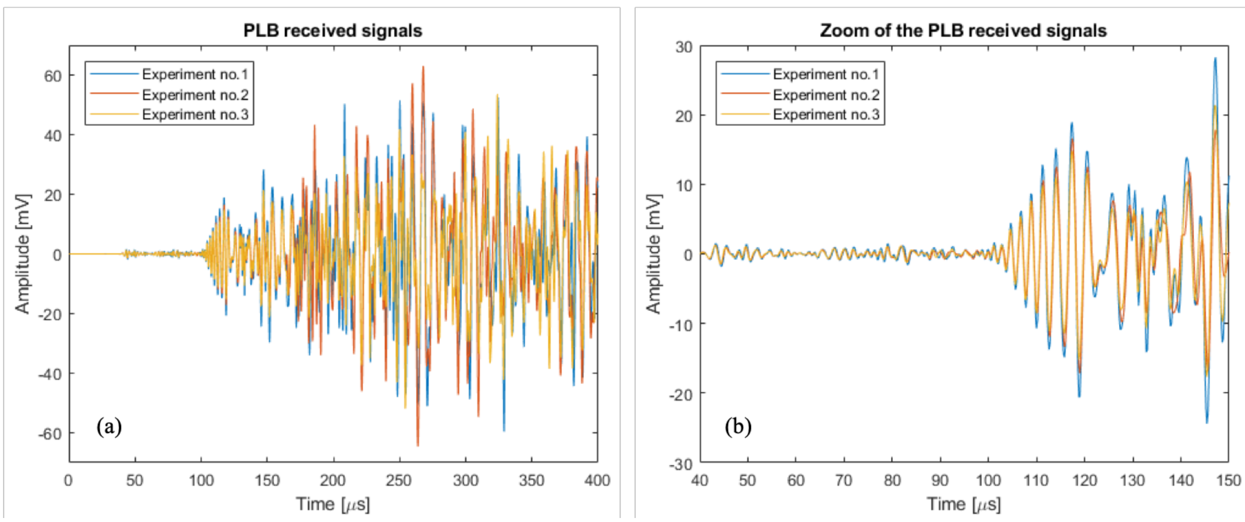

Fig. 5: Plot of the received PLB signals from 0 μs to 400 μs, (a), from 40 μs to 150 μs, (b).

In Fig. 5 (b) is reported a zoom view of the recorded signals in the time interval between 40 μs and 150 μs. The three experiments are quite similar at the beginning whereas they start to diverge after 120 μs. The chosen distance was great enough to appreciate the mode separation. Indeed, the threshold crossing at 40 μs is due to the S_0 mode while the A_0 mode arrives later at around 100 μs.

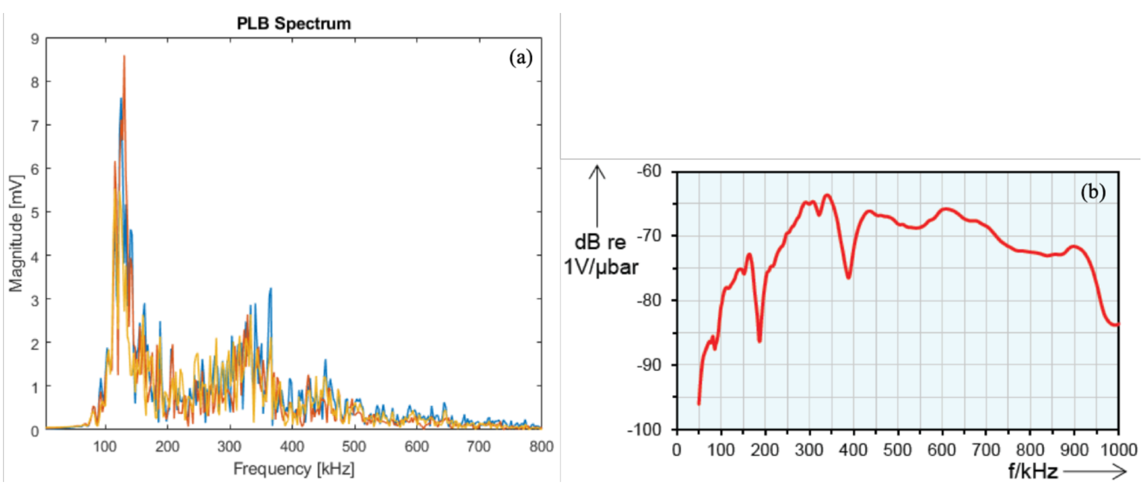

Fig. 6: Fourier transform of the three PLB tests, (a), piezoelectric sensor VS900-M frequency response, (b).

The spectrum analysis has been performed doing the Fourier transform of the recorded signals and it is represented in Fig. 6 (a). The energy is not distributed in uniformly along all the frequencies but is concentrated mainly between 100 kHz and 150 kHz. Moreover, it is interesting to compare this spectrum with respect to the piezoelectric sensor response in Fig. 6 (b). The VS900-M is a broadband frequency sensor with characteristic anti-resonances at 200 kHz and 400 kHz. Therefore, the spectrum of the received signal is somehow filtered due to this sensor response. Indeed, the two anti-resonances are also visible in the frequency domain of the received signal. Nevertheless, the low amount of energy in all the other frequencies greater than 150 kHz cannot be due to the sensor response that has peaks both at 190 kHz and 350 kHz. As such, the spectrum is not filtered just by the sensor response, but more properly by the system plate-sensor. For the aforementioned considerations, this phase of the research project, it was assumed that the energy associated to the PLB spectrum is mainly concentrated around 130 kHz. This hypothesis is required to assess the Lamb waves group velocities since they are frequency dependent.

VII. Group velocity estimation

Building an efficient localization algorithm is essential in the context of SHM. It can provide to engineers the source of the acoustic emission location generated by a crack or another kind of material failure mechanism. Typically, localization algorithms exploit triangulation techniques based on the TOA recorded at different transducers attached to the monitored structure. The prediction of the source location is linked to the TOA at the different transducers and the characteristic wave velocity in the considered medium. While the TOA parameter is simply recorded by the sensors and directly available for the user, the speed of sound has to be determined.

The group velocity estimation is directly involved in the location algorithm performance since it is used to convert TOA differences into distances from the source location. In this study, it was referred to the analytical model of Lamb waves and then the results were compared with the ones obtained in the experiments.

A. Analytical approach

The Vallen Systeme provides a software able to plot the dispersion curves of Lamb waves given the longitudinal wave speed c_p, the shear wave speed c_s and plate thickness d. Aluminum 7075-T651 has typical c_p and c_s values of 6148 m/s and 3097 m/s respectively. The dispersion curves are shown in Fig. 7.

Considering the fact that the spectrum is characterized by a strong peak at 130 kHz, it is possible to use the dispersion curves of Fig. 7 to assess the group velocities of the different modes at that frequency. Firstly, one can observe that only the fundamental symmetric and antisymmetric Lamb wave modes are present at 130 kHz.

The localization algorithm provided by the Vallen Systeme uses as reference for the TOA the first threshold crossing. Therefore, with the selected threshold value, this TOA will be related to the fastest mode recorded by the piezoelectric sensor. From Fig. 7 it is clear that the S_0 is much faster with respect the A_0 in all the frequency range associated with a PLB experiment. In particular, at 130 kHz this analytical model associates a value for the S_0 equal to 5341 m/s. Moreover, the S_0 has a group velocity with a much more stable value, up to 500 kHz, with respect the A_0. The plateau in the range [0-500 kHz] of the S_0 mode group velocity, appreciable in Fig. 7, makes it suitable for the localization algorithm even if the frequency is not purely constant since it would produce just a slight change in the estimated group velocity.

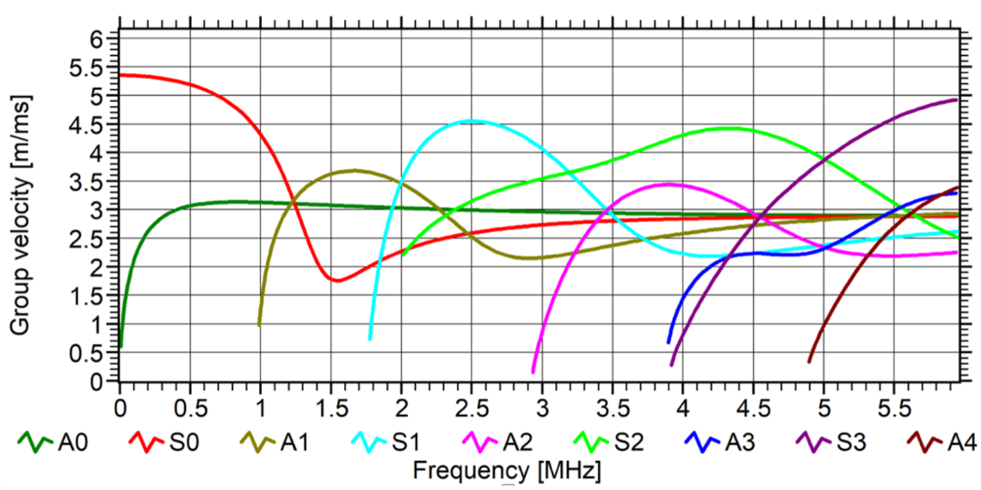

Fig. 7: Dispersion Curves

B. Experimental approach

The previous obtained result must find confirmation in the experimental results. The same experiment used for the spectrum characterization was also used to assess the S_0 velocity. Sensor 1 is aligned with the PLB source and Sensor 6 (they have the same X coordinate). This means that it is possible to determine the speed of the S_0 mode simply by dividing the TOA difference, recorded at two transducers, by the relative distance between them. The latter can be computed from the reading of Table 1, providing a value for the distance equal to 244.9 mm.

The recorded TOA are reported in Table 2, where the S_0 mode velocity and the percentage error with respect to the result of 5341 m/s derived from the analytical model utilizing the Vallen software is also computed. The TOA are related to the threshold crossing of the closest sensor to the AE source. Hence, in this case they are referred taking as zero TOA the threshold crossing in Sensor 4.

Table 2. TOA and S_0 velocity computation

Exp. no.	TOA [μs]		Δ TOA [μs]	d [mm]	S_0 Speed [m/s]	% Error
	CH. 1	CH. 8	CH. 8-1	CH. 8-1	CH. 8-1	CH. 8-1
1	21.2	67.9	46.7	244.9	5244.1	-1.85
2	21.7	68.2	46.5	244.9	5266.7	-1.41
3	21.1	67.7	46.6	244.9	5255.4	-1.63

Taking an average between the three experiments one obtains the group velocity related to the S_0 mode, equal to 5255,4 m/s. The speed derived from the experiment is slightly lower than the one computed analytically (5341 m/s), precisely 1.63% slower. However, this result is still consistent with the theory. Indeed, the analytical models does not consider the wave attenuation due to damping. A decrease in amplitude due to damping (both geometrical and structural) affects the threshold crossing, shifting the TOA of few microseconds later and, consequently, only apparently decreasing the expected speed. Decreasing the threshold crossing can reduce this error with the drawback to be more sensitive to background noise.

VIII. Localization algorithm

The computed S_0 velocity is now used in the localization algorithm set-up. Table 3 reports the coordinates where the PLB tests were performed. In each location, four PLB experiments with a 0.3 mm lead at 45 degrees where performed. The recorded signals have been analyzed applying the location processor followed by the application of the location uncertainty filter.

Table 3. PLB test location layout

Test	Coordinates [mm]		Coordinates [in.]	
	X	Y	X	Y
PLB 1	76.2	152.4	3	6
PLB 2	101.6	406.4	4	16
PLB 3	228.6	457.2	9	18
PLB 4	203.2	203.2	8	8

A. Location Processor

The Vallen System provides a localization algorithm based on the difference of the TOA related to each sensor. In particular, to every TOA difference, related to a pair of sensors, corresponds a certain distance computed multiplying that TOA difference by the user defined velocity which in this case is 206.9 in./ms. This translates to the generation of a hyperbola for each couple of sensors. Indeed, a hyperbola is defined as the set of all points such that the difference of the distances between any point and the foci is constant. In this kind of application, the two foci are the pair of piezoelectric transducers. The source location could lie in every point belonging to the hyperbola. The intersection of different hyperbole produces the predicted source location. As an example, in Fig. 8 the aforementioned processor is applied to identify one of the four sources (PLB 4) of the experiment. For a planar problem, a minimum number of three sensors is required to determine the source location. This is shown by Eq. (5), which represents the time difference of arrival function [11]:

$$\Delta t_i = \frac{\sqrt{(x_i-x)^2+(y_i-y)^2}-\sqrt{(x_1-x)^2+(y_1-y)^2}}{v_g} \tag{5}$$

Where x and y represent the AE source coordinates to be determined, x_i and y_i symbolize the *i*th sensor coordinates and v_g is the group velocity of the propagating wave. Since Eq. (5) has two unknowns and one sensor has to be used as reference, a minimum number of three sensors is required to solve the localization problem.

When more than three sensors are used, the system of equations, representing the time difference of arrival functions, is over determined, leading to regression analysis approaches [12]. This set of non-linear equations can be solve by means of both non-iterative and iterative schemes. The Vallen Systeme makes used of the Geiger's method [13], which is an iterative scheme requiring an initial guess value for the source location (usually set automatically with the location of the first hit sensor).

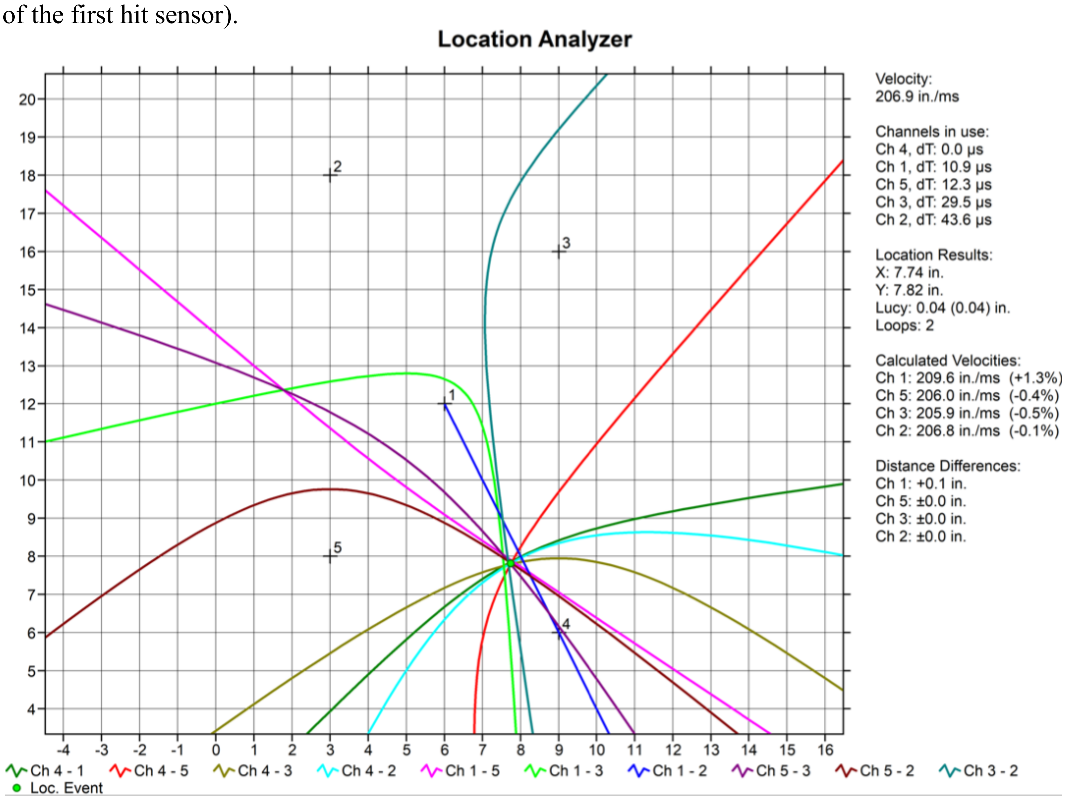

Fig. 8: Example of the Localization analyzer processor

B. LUCY Filter

External disturbances, undesired reflection, poor accuracy in the experiment execution are all factors that can lead to potentially wrong results. Therefore, the data have to be further filtered and this is done by means of the LUCY filter (location uncertainty) provided by the developer [10].

The Localization Uncertainty (LUCY) can be considered a measure of the source position accuracy with respect the measured TOA differences. It consists in the standard deviation from a set of *measured* values D_i to a set of *calculated* values P_i. Its expression is represented by Eq. 6:

$$LUCY = \sqrt{\sum_{i=2}^{n}(D_i - P_i)^2/(n-1)} \tag{6}$$

Where index "i" represents the i-th hit sensor. D_i is computed multiplying the *measured* TOA difference with respect the first hit sensor by the user defined speed of sound. On the other hand, P_i identifies the distance computed multiplying the *calculated* TOA difference by the previous defined speed of sound. In particular, the *calculated* TOA difference refers to the result of the computed source position. Then a result was considered valid only for LUCY values lower than 0.3 inches. The choice of the threshold for the LUCY parameter is arbitrary and has to be defined by the user in such a way the wrong results are filtered without discarding also the right ones.

IX. Results and Discussion

The results are summarized in Fig. 9 where the case without the application of the LUCY filter (a), is compared with the case in which, controversially, the filter is applied (b). The red crosses, measuring 1 inch by 1 inch, highlight the PLB test locations reported in Table 3. Around every PLB test location a relative high number of hits is recorded but, in Fig. 9 (a) would be impossible to assess in an objective way the right source location. The reason could lay in wave reflections coming from the edges. Those waves interact with the original signal and create new hits on the sensors. Nevertheless, an incredible improvement can be achieved applying the LUCY filter imposing a threshold value of 0,3 inches as shown in Fig. 9 (b). All the wrong estimated points are successfully filtered, highlighting the correct source locations applied in the experimental setup. Moreover, the sensors layout seems to have an influence on the efficiency of the localization algorithm. Their configuration is not symmetric with respect the AE source locations due to the presence of the extra Sensor 6 (Channel 8) in the upper plate portion. As such, the PLB tests performed in the upper half of the plate are better estimated by the localization algorithm than the others. This can be appreciated observing that in Fig. 9 (b) they are almost centered with respect their relative red cross. On the other hand, the PLB tests performed in the south region of the plate are slightly shifted toward the south-west direction. Therefore, the presence of one extra sensor improves the algorithm performance for the PLB sources located close to the sensor itself. This finds confirmation considering that the Geiger's method performance decreases moving outward the region enclosed by the sensors [11]. Thanks to the results provided by the localization algorithm it is possible to modify the previous computed speed of sound in such a way that the LUCY parameter was minimized. This leads to an iterative process which used as first guess value the speed computed from the reading of the dispersion curves verified experimentally. At the end of the iterative process, the optimized velocity value for the S_0 mode has been slightly reduced from 206,9 in./ms to 206.5 in./ms (5245.1 m/s in metric units). The value corresponds to the 98.2% of the predicted value according to the dispersion curves related to specimen material and geometry.

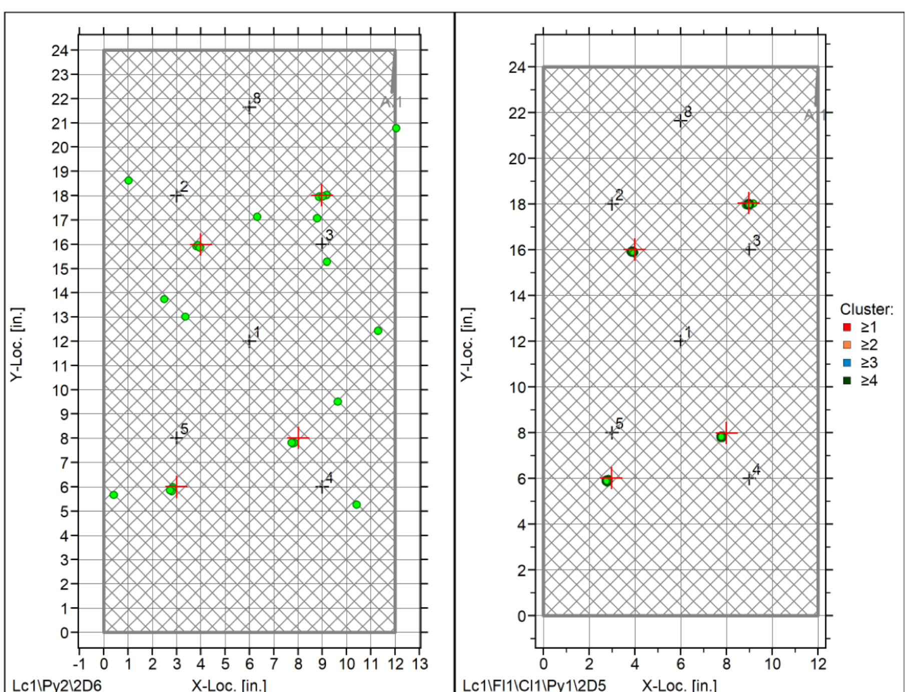

(a) (b)

Fig. 9: Experimental results: unfiltered (a) and filtered using LUCY algorithm (b)

X. Conclusion

In this paper a methodology for the calibration of an AE localization algorithm was derived. The applied procedure consisted in determining the right threshold value, characterizing the signal in the frequency domain, computing the corresponding S_0 group velocity from the analytical model and comparing the result with experimental data. This velocity was used as input for the localization algorithm, selecting a proper value for the uncertainty location filter. Finally, the obtained S_0 group velocity was modified such that the LUCY parameter was minimized. This led not only to a calibrated localization algorithm for SHM applications, but also to a methodology able to assess the true group velocity value of the symmetric mode in the analyzed structure. The latter point is currently of particular interest to calibrate FEM models which can be used to model Lamb waves propagation. Moreover, the use of FEM models can open the possibility to reconstruct useful signal features by means of time reversal techniques in order to distinguish different types of AE sources and hence different types of possible damages. Nevertheless, future research activity is required to apply a similar methodology to composite material which do not show isotropic material properties and therefore require a different kind of localization algorithm.

Acknowledgements

This study would have been impossible without the extraordinary support of Prof. Enrico Troiani for encouraging me in this challenge, putting me in contact with his colleagues at Clarkson University. The author would like to thank also Prof. Marcias Martinez for his expert advice, continuous guidance and passion.

References

[1] C. R. Farrar, K. Worden, "An introduction to structural health monitoring," *Philosophical Transactions of the Royal Society A Mathematical Physical and Engineering Sciences,* Vol. 365, No. 1851, 2007, pp. 303, 315.
[2] D. Balageas, C. Fritzen, A. Güemes, *Structural Health Monitoring*, ISTE, 2006.
[3] ASTM E-976, *Standard Guide for Determining the Reproducibility of Acoustic Emission Sensor Response,* ASTM International.
[4] M. Hamstad, "Acoustic emission signals generated by monopole (pencil-lead break) versus dipole sources: finite element modeling and experiments," *Journal of Acoustic Emissions,* Vol. 25, 2007, pp. 92, 106.
[5] H. Lamb, "On Waves in an Elastic Plate," *Proceedings of the Royal Society,* Vol. 93, No. 648, 1917.
[6] J. Rose, *Ultrasonic Guided Waves in Solid Media*, Cambridge University Press, 2014.
[7] K. Worden, "Rayleigh and Lamb Waves - Basic Principles," *Strain,* Vol. 37, No. 4, 2001, pp. 167, 172.
[8] C. Sbarufatti, G. Manson, K. Worden, "A numerically-enhanced machine learning approach to damage diagnonis using Lamb wave sensing network," *Journal of Sound and Vibration,* Vol. 333, 2014, pp. 4499, 4525.
[9] D. Aljets, A. Chong, S. Wilcox, K. Holford, "Acoustic emission source location on large plate-like structures using a local triangular sensor array," *Mechanical Systems and Signal Processing,* Vol. 30, 2012, pp. 91, 102.
[10] Vallen-Systeme GmbH, *AMSY-6 Operation Manual,* Icking: Vallen-Systeme GmbH, 2017.
[11] M.J.G.N. Boon, "Temperature and Load Effects in Modelling and Experimental Verification of Acoustic Emission Signals for Structural Health Monitoring Applications," M.Sc.Dissertation, Faculty of Aerospace Engineering, Delft University of Technology, 2014.
[12] M. Ge, "Analysis of source location algorithms, Part I: Overview and non-iterative methods," *J. Acoustic Emission*, Vol. 21, 2003, pp. 14, 28.
[13] M. Ge, "Analysis of source location algorithms, Part II: Iterative methods," *J. Acoustic Emission*, Vol. 21, 2003, pp. 29, 51.